Journal of Chromatography A, 1217 (2010) 7131–7137

Contents lists available at ScienceDirect

Journal of Chromatography A

journal homepage: www.elsevier.com/locate/chroma

The obstruction factor in size-exclusion chromatography. 1. The intraparticle obstruction factor

Dustin J. Richard, André M. Striegel*

Department of Chemistry & Biochemistry, Florida State University, Tallahassee, FL 32306-4390, USA

ARTICLE INFO

Article history:
Received 9 June 2010
Received in revised form 27 August 2010
Accepted 8 September 2010
Available online 17 September 2010

Keywords:
Obstruction factor
Intraparticle obstruction
Mass transfer
Size-exclusion chromatography
Packed column chromatography

ABSTRACT

We report the first of a series of studies on the obstruction factor γ in size-exclusion chromatography (SEC). Here, using narrow dispersity polymer standards we examine how the intraparticle obstruction factor γ_p depends individually on a number of analyte properties, column characteristics, and user-defined parameters. Far from being constant, γ_p is seen to vary with analyte molar mass and solvent, as well as with the pore size and particle size of the column packing material, sometimes in seemingly counterintuitive manner. Over the limited temperature range accessible to our equipment, however, no statistically significant change in γ_p with temperature was discovered. The results presented should be applicable to forms of packed column chromatography other than SEC. The latter technique, however, presents a convenient test bed for quantitative determination of the obstruction factor, due to minimized sorptive mass transfer and longitudinal diffusion contributions to band broadening in most forms of SEC.

1. Introduction

In 1956, van Deemter et al. first identified three different fundamental causes of band broadening in chromatography [1], namely eddy diffusion (*A*-term), longitudinal diffusion (*B*-term), and resistance to mass transfer (*C*-term), which were incorporated into the now-classic van Deemter equation, given in expanded form in Eq. (1) [2]:

$$H = A + \frac{B}{\nu} + C_M\nu + C_{SM}\nu + C_S\nu \quad (1)$$

where H is the plate height; ν is the flow velocity of the mobile phase; C_M is the resistance to mass transfer that occurs in the interstitial mobile phase, i.e., between the particles of column packing material; C_{SM} is the intraparticle mass transfer, i.e., the resistance to mass transfer in the stationary phase or, in the case of size-exclusion chromatography (SEC), in the stagnant mobile phase inside the pores of the column packing material; and C_S is the resistance to mass transfer due to sorptive–desorptive (i.e., enthalpic) interactions between the analyte and the column packing material.

The research presented here focuses on the mass transfer (*C*) terms of the van Deemter and related equations. Because the primary form of band broadening in non-oligomeric size-exclusion chromatography is resistance to mass transfer [2], we use SEC to isolate a particular component of the *C* term, namely the intraparticle obstruction factor, γ_p, defined as the ratio of the diffusion coefficient of the analyte within the pores of the packing material to the diffusion coefficient of the analyte in the flowing mobile phase.

In the present experiments, we have determined γ_p under a variety of experimental conditions and examine how various analyte properties, column characteristics, and user-defined parameters affect this term. We compare the effect on γ_p of analyte properties such as molar mass and repeat unit chemistry, of experimental parameters such as solvent and temperature, and of column properties such as particle size and pore size.

2. Background

The diffusion coefficient of an analyte in free solution or traveling through an open tube depends on solvent, temperature, and analyte molar mass. If this same analyte travels through a column packed with porous, non-interacting particles, both tortuosity (the "zig–zag" network of channels throughout the packed medium) and constriction (the widening and narrowing of these channels) cause the diffusion coefficient of the analyte to appear to be smaller than in the open tube, free solution scenario under otherwise identical conditions [3]. For a given analyte, this difference in diffusion coefficients is known as the obstruction factor γ, or total obstruction factor γ_t, and is defined as:

$$\gamma_t = \frac{D_{eff}}{D_m} \quad (2)$$

where D_{eff} is the effective or apparent diffusion coefficient of an analyte in a packed column and D_m is the diffusion coefficient

* Corresponding author. Tel.: +1 850 942 0362; fax: +1 850 644 8281.
E-mail address: striegel@chem.fsu.edu (A.M. Striegel).

0021-9673/$ – see front matter © 2010 Elsevier B.V. All rights reserved.
doi:10.1016/j.chroma.2010.09.021

of the same analyte in free solution or in an open tube. For an open tube, in which diffusion is unobstructed, $\gamma_t = 1$, whereas for a maximally obstructed scenario $\gamma_\tau = 0$ (i.e., larger values of the obstruction factor correspond to less obstruction to diffusion). In the case of porous media in a chromatographic column, not only does obstruction occur as the analyte travels in the interstitial space between the column particles (interparticle obstruction), but also as a result of permeation within the pores of the column packing (intraparticle obstruction). The former case is described by the interparticle obstruction factor γ_e, the latter by the intraparticle obstruction factor γ_p.

The work presented here focuses on the intraparticle obstruction factor γ_p. We use SEC to determine if and how γ_p varies with changes in analyte and column properties as well as with changes in user-controlled parameters. Our choice of SEC is based on two major considerations. First, outside of the oligomeric region longitudinal diffusion has a negligible effect on chromatographic band broadening in SEC [4], meaning that the B term in Eq. (1) should not significantly influence our results. Second, due to the entropic nature of SEC separations (verified experimentally; also, see *e.g.* [5,6]), we need not worry about mass transfer processes resulting from enthalpically-governed sorption–desorption processes between the analyte and the packing material (the C_S term in Eq. (1)).

The most significant form of chromatographic band broadening in non-oligomeric SEC is mass transfer via intra- and interparticle diffusion. With eddy diffusion (A-term) processes generally considered to be flow-rate-independent (or weakly dependent), it should therefore be possible to isolate the effect(s) of stagnant mobile phase (C_{SM}) mass transfer processes on γ_p.

Even with the growing use of on-line static light scattering detectors [2,7–9], the most common method of determining the molar mass of polymers using SEC remains peak-position calibration curves. Because these curves rely on a logarithmic M scale, small changes in peak width can correspond to large differences in molar mass. Band broadening will thus lead to underestimation of the lower statistical moments of the molar mass distribution (MMD) of a polymer ($M_n, M_{n-1}, \ldots$), to overestimation of the higher moments (M_w, M_z, M_{z+1}, ...), and to a belief that the MMD itself covers a broader M range than it, in fact, does. To effect more accurate band broadening corrections than currently exist (see *e.g.*, Section 8.7 in Ref. [2]), in both size-based and "interactive" separation techniques [10,11], we rely on an increased fundamental understanding of the mechanisms responsible for band broadening and of their consequences.

Dating back to the work of Giddings in the mid-1960s, various theories have been proposed to describe the complex effects of solute diffusion within porous materials, in general, and the role of the intraparticle obstruction factor, in particular [3,12–16]. In 1981, Klein and Grüneberg used Eq. (3) as the basis through which to measure intraparticle obstruction [14]:

$$\sigma^2_{\text{perm}} = \frac{K_{SEC} V_i d_p^2 u}{30 D_s} = \frac{K_{SEC} V_i d_p^2 u}{30 \gamma_p D_m} \tag{3}$$

where σ^2_{perm} is the variance of the peak due to solute permeation into and out of the pores of the packing material; K_{SEC} is the solute distribution coefficient, the ratio of the analyte concentration in the stationary phase (internal pore volume or stagnant mobile phase) to that in the mobile phase (interstitial volume); V_i is the internal pore volume; d_p is the particle diameter; u is the volumetric flow rate; and D_s is the effective diffusion coefficient in the stationary phase. The structural size parameter of 1/30 was derived based on the very realistic assumption that the shape of the packing material is spherical [3].

Eq. (2) can be written in terms of intraparticle obstructivity γ_p and intraparticle effective diffusion D_s as:

$$\gamma_p = \frac{D_s}{D_m} \tag{4}$$

We account for obstruction within the pores only by examining the fraction of analyte that permeates into the pores, as given by K_{SEC}. For analytes experiencing only interparticle obstruction, represented by the factor γ_e, $K_{SEC} = 0$ and a different equation is used. We deal with this in an upcoming publication.

The internal pore volume V_i in Eq. (3) is determined via:

$$V_i = V_{\text{Total}} - V_o \tag{5}$$

where V_{Total} is the retention volume of a totally permeating solute (i.e., of a small solute that samples all available interstitial and pore volume), and V_o is the void volume for an unretained solute (i.e., of a large solute which cannot penetrate the pores of the packing material and which, therefore, samples only the interstitial volume). In SEC, the partition coefficient K_{SEC} of an analyte is calculated according to [2,17]:

$$K_{SEC} = \frac{V_R - V_o}{V_i - V_o} \tag{6}$$

where V_R is the retention volume of the analyte. By performing experiments at several flow rates, measuring the change in peak variance as a function of flow rate (i.e., measuring $\partial\sigma^2_{\text{perm}}/\partial u$), and rearranging Eq. (3), one obtains:

$$\gamma_p = \frac{K_{SEC} V_i d_p^2}{30 D_m (\partial\sigma^2_{\text{perm}}/\partial u)} \tag{7}$$

The non-constant terms of Eq. (7), namely K_{SEC}, V_i, and $\partial\sigma^2_{\text{perm}}/\partial u$, can be determined experimentally, V_i and K_{SEC} through Eqs. (5) and (6), respectively, and $\partial\sigma^2_{\text{perm}}/\partial u$ from the slope of a plot of variance versus flow rate. The parameters that remain constant in Eq. (7) are d_p, the average packing particle diameter, provided by the column manufacturer, and D_m, the solute diffusion coefficient, which is constant for a particular molar mass of a given analyte in a given solvent at a given temperature. For large M polymers, which diffuse orders of magnitude more slowly in solution than their monomeric or oligomeric counterparts, measuring the change in variance with changing flow rate is preferred to the so-called "stop–flow" method, which measures the change in variance as a function of the time during which an analyte is held on the column at zero flow [4,16]. The latter type of experiments are essentially inapplicable (or, at least, highly impractical) when it comes to polymers with M greater than about 30,000 g/mol.

Here, we have employed Eq. (7) to determine γ_p. Our intent has been to isolate the dependence of γ_p on various user-defined parameters, packing material characteristics, and sample properties. We have done this by using the relation between γ_p and the flow rate dependence of the band broadening that occurs during SEC analysis of different polymers (namely, polystyrene and poly(methyl methacrylate)), while individually varying molar mass, solvent, temperature, column pore size, and packing material diameter. Enthalpic contributions to the separations presented are negligible and, with the possible exception of some of the lower M polymers examined, our results should be absent of any substantial contribution from longitudinal diffusion [4]. Because the contributions to band broadening from both A-term eddy diffusion and molar mass dispersity are constant and thus cancel out when measuring the *change* in band broadening as a function of flow rate [16], and the B-term and C_S-term contributions to band broadening are minimal, our experiments aim to quantitatively isolate the remaining C-term contribution to γ_p. Results should be applicable to forms of liquid chromatography other than SEC, as well as

to improved understanding of diffusion through porous media in general [18,19].

3. Experimental

3.1. Materials

Tetrahydrofuran (THF), spectrophotometric grade, inhibited with 250 ppm butyrated hydroxytoluene, was purchased from EMD Chemicals (Gibbstown, NJ, USA); chloroform was purchased from BDH (West Chester, PA, USA); and toluene was purchased from Fisher Scientific (Fair Lawn, NJ, USA).

Polystyrene (PS) of molar masses 355,000 g/mol and 1,260,000 g/mol were purchased from Toyo Soda Manufacturing Company (Tokyo, Japan). Poly(methyl methacrylate) (PMMA) of molar masses 467,000 g/mol and 838,300 g/mol were purchased from Scientific Polymer Products (Ontario, NY, USA) and of molar mass 1,500,000 g/mol from American Polymer Standards Corporation (Mentor, Ohio, USA). All other standards were from Agilent/Polymer Laboratories (Amherst, MA, USA). Molar mass information given in the tables and throughout the paper was provided by the manufacturers. For all PS and PMMA standards, molar mass dispersity $M_w/M_n \leq 1.1$. All columns were from Agilent/Polymer Laboratories.

3.2. Chromatography

All experiments were performed using 1 mg/mL solutions of PS and PMMA in either THF or $CHCl_3$, a concentration 2–6 times lower than the critical overlap concentration c^* of even the highest M PS and PMMA examined. Each polymer was added to the solvent, gently shaken, and allowed to solvate overnight. To each 2 mL injection vial, 5 μL of toluene was added to determine the total permeation volume of the column and also to act as a reference peak serving to adjust for minor pump fluctuations. Two unretained polymers, 1,260,000 g/mol PS and 1,500,000 g/mol PMMA, were used to determine the void volume V_o of the 10^4 Å pore size columns. The void volume of the 10^5 Å pore size column was determined with a 4,400,000 g/mol PS.

Three commercially-available PLgel columns were used individually for each experiment: a 10 μm particle size, 10^4 Å pore size column; a 5 μm particle size, 10^4 Å pore size column; and a 10 μm particle size, 10^5 Å pore size column. Information provided by the manufacturer indicated the actual average particle size for the columns is closer to 8 μm and 4 μm for the 10 μm and 5 μm columns, respectively. As such, we used the former values (8 and 4 μm) rather than the latter ones (10 and 5 μm) in all calculations of γ_p.

100 μL of each polymer solution were injected onto each column, at a flow rate of 1 mL/min using a Waters 2695 Separations Module (Waters, Milford, MA, USA). The concentration of the analytes was detected using a Waters 410 differential refractometer (Waters). For all experiments, the temperature of the sample, injector, and column compartments and the detector temperature were maintained at 30 ± 1 °C. This procedure was then repeated at flow rates of 0.75, 0.50, 0.30, and 0.15 mL/min for PS in both THF and $CHCl_3$ and for PMMA in THF. None of the polymers appeared to degrade during analysis.

For data acquisition and for determination of peak variances, we used Clarity software (version 2.4.1.91) from DataApex (Prague, Czech Republic) and Origin Peak Fitting Module software (v.1.4) from OriginLab (Northampton, MA, USA), respectively. For molar masses below 500,000 g/mol, a Gaussian fit was used for determination of the peak variance, while for molar masses 500,000 g/mol and above, an exponentially-modified Gaussian (EMG) equation [2,20–22] was used due to the larger peak tailing that occurred for the higher molar mass samples. This tailing is expected, as the living anionic polymerization used to make narrow-polydispersity PS and PMMA samples yield polymers with a Poisson-like distribution [23] (an additional source of tailing for the highest M polymers in the 10^4 Å columns is that a significant number of molecules may not enter the pores of the column packing material when $K_{SEC} \approx 0$ [24]).

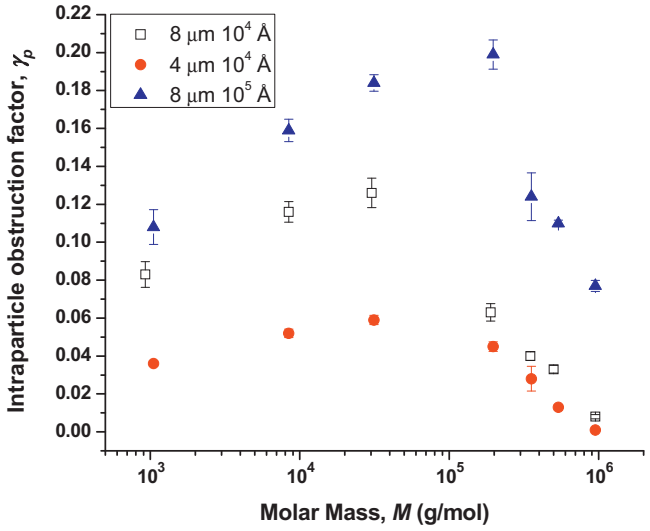

Fig. 1. Effect of molar mass, particle size, and pore size on the intraparticle obstruction factor γ_p of PS in THF at 30 °C.

Separation appeared to follow a near-ideal size-exclusion mechanism, i.e., was primarily governed by entropic, not enthalpic interactions between the analyte and the stationary phase. This conclusion was arrived at by determining the K_{SEC} of the various PS and PMMA standards used at two different temperatures, 30 and 50 °C. With this 20 °C change in temperature, the biggest change in K_{SEC} observed was only 2% and, in most cases, the change was <1%. Had there been a substantial enthalpic contribution to the separation, we would have expected a much larger change in K_{SEC} (on the order of 10–20% or more) with a 20 °C change in temperature [6,25,26].

4. Results and discussion

4.1. Determination of γ_p

Results from our experiments are shown in Tables 1–3 and Figs. 1–3. In all cases, the intraparticle obstruction factor γ_p was determined according to Eq. (7). The distribution coefficient K_{SEC} was obtained from Eq. (6). The total exclusion volume V_o was determined as described in Section 3.2. The pore volume V_i was the difference between V_o and the retention volume of toluene, a totally permeating solute (identical results were obtained using acetone in select injections).

For the remaining parameters in Eq. (7), for d_p we used the particle diameters provided us by the manufacturer which, as noted in the previous section, are approximately 20% smaller than the values in product brochures. The peak variances σ^2 at the various flow rates u were determined using either a Gaussian or an EMG fit, as explained in Section 3.2.

Values for D_m were obtained from previously-determined relationships at 25 °C (adjustment for temperature differences is explained at the end of this section). For PS in THF, D_m were

Table 1
Intraparticle obstruction factor (γ_p) values for PS and PMMA at both 30 and 50 °C for a 8 μm particle size, 10^4 Å pore size column.

THF					$CHCl_3$		
Polystyrene			Poly(methyl methacrylate)		Polystyrene		
Molar mass (g/mol)[a]	γ_p		Molar mass (g/mol)	γ_p (30 °C)	Molar mass (g/mol)	γ_p	
	30 °C	50 °C				30 °C	50 °C
925	0.083 (0.007)[b]	0.079 (0.007)	1280	0.081 (0.007)	1050	0.096 (0.006)	0.098 (0.005)
8450	0.116 (0.005)	0.109 (0.005)	4910	0.110 (0.007)	8450	0.119 (0.004)	0.122 (0.015)
30,300	0.126 (0.008)	0.126 (0.006)	27,000	0.090 (0.005)	31,420	0.116 (0.002)	0.112 (0.007)
189,300	0.063 (0.005)	0.063 (0.002)	107,000	0.072 (0.002)	197,300	0.047 (0.005)	0.061 (0.032)
355,000	0.040 (0.002)	0.041 (0.003)	265,000	0.023 (0.001)	355,000	0.033 (0.001)	0.032 (0.002)
500,000	0.033 (0.002)	0.028 (0.002)	467,000	0.022 (0.002)	538,000	0.011 (0.001)	0.023 (0.002)
950,000	0.008 (0.001)	0.007 (0.002)	838,300	0.006 (0.001)	950,000	0.011 (0.005)	0.012 (0.006)

[a] Peak-average molar mass, M_p, as provided by manufacturer.
[b] Data in parentheses represent standard deviations based on at least triplicate analyses. See Section 3 for details.

Table 2
Intraparticle obstruction factor (γ_p) values for PS and PMMA at 30 °C for a 4 μm particle size, 10^4 Å pore size column.

THF				$CHCl_3$	
Polystyrene		Poly(methyl methacrylate)		Polystyrene	
Molar mass (g/mol)[a]	γ_p (30 °C)	Molar mass (g/mol)	γ_p (30 °C)	Molar mass (g/mol)	γ_p (30 °C)
1050	0.036 (0.001)[b]	1280	0.045 (0.004)	1050	0.023 (0.001)
8450	0.052 (0.002)	4910	0.044 (0.003)	8450	0.032 (0.002)
31,420	0.059 (0.002)	30,530	0.050 (0.003)	31,420	0.034 (0.002)
197,300	0.045 (0.003)	90,250	0.047 (0.004)	197,300	0.033 (0.003)
355,000	0.028 (0.007)	342,900	0.016 (0.003)	355,000	0.018 (0.001)
538,000	0.013 (0.001)	467,000	0.010 (0.002)	538,000	0.009 (0.001)
950,000	0.001 (0.001)	838,300	0.003 (0.001)	950,000	0.006 (0.001)

[a] Peak-average molar mass, M_p, as provided by manufacturer.
[b] Data in parentheses represent standard deviations based on at least triplicate analyses. See Section 3 for details.

obtained from [27]:

$$D_m = (2.4 \pm 0.1) \times 10^{-4} M^{(0.54 \pm 0.01)} \quad (8)$$

and for PMMA >30,000 g/mol from [28]:

$$D_m = 2.3 \times 10^{-4} M^{-0.517} \quad (9)$$

where M is the molar mass of the analyte. For PMMA <30,000 g/mol, D_m were determined by comparison to the D_m versus M relationships obtained by Yamakawa et al. in acetonitrile [29], which extended into the oligomeric region of PMMA. Conveniently, for $M \geq$30,000 g/mol the slope of a plot of D_m versus M for PMMA in THF is equal to that of the same plot for PMMA in acetonitrile. As such, we used this constant offset between each set of plots, in combination with Eq. (9), to obtain the D_m in THF of PMMA with M < 30,000 g/mol (applying a similar procedure to PS < 30,000 g/mol yielded D_m that very closely matched those measured by Wernert et al. in reference [27]).

For PS in $CHCl_3$, D_m was obtained using the relation [30]:

$$D_m = 1.24 \times 10^{-4} M^{-0.492} \quad (10)$$

Adjustment for differences in temperature (50 or 30 °C experimental temperatures versus 25 or 20 °C literature reference temperatures) was done via [31]:

$$D_{m,exp} = D_{m,ref} \left(\frac{T_{\exp}}{T_{ref}} \right) \left(\frac{\eta_{ref}}{\eta_{\exp}} \right) \quad (11)$$

where $D_{m,exp}$ were the values we used in our calculations at an absolute temperature (in Kelvin) T_{exp} in a solvent of viscosity η_{exp}, and comparison was to D_m values from the literature ($D_{m,ref}$) obtained at an absolute temperature T_{ref} in a solvent of viscosity η_{ref}.

4.2. Effect of molar mass on γ_p

As can be seen in Tables 1–3 and Figs. 1–3, the intraparticle obstruction factor is molar-mass-dependent, with this dependence

Table 3
Intraparticle obstruction factor (γ_p) values for PS and PMMA at 30 °C for a 8 μm particle size, 10^5 Å pore size column.

THF				$CHCl_3$	
Polystyrene		Poly(methyl methacrylate)		Polystyrene	
Molar mass (g/mol)[a]	γ_p (30 °C)	Molar mass (g/mol)	γ_p (30 °C)	Molar mass (g/mol)	γ_p (30 °C)
1050	0.108 (0.009)[b]	1280	0.129 (0.013)	1050	0.132 (0.015)
8450	0.159 (0.006)	4910	0.097 (0.004)	8450	0.145 (0.007)
31,420	0.184 (0.004)	32,530	0.146 (0.006)	31,420	0.149 (0.020)
197,300	0.199 (0.008)	90,250	0.144 (0.008)	197,300	0.119 (0.028)
355,000	0.124 (0.013)	342,900	0.082 (0.003)	355,000	0.099 (0.008)
538,000	0.110 (0.002)	467,000	0.074 (0.008)	538,000	0.069 (0.006)
950,000	0.077 (0.003)	838,300	0.037 (0.005)	950,000	0.041 (0.009)

[a] Peak-average molar mass, M_p, as provided by manufacturer.
[b] Data in parentheses represent standard deviations based on at least triplicate analyses. See Section 3 for details.

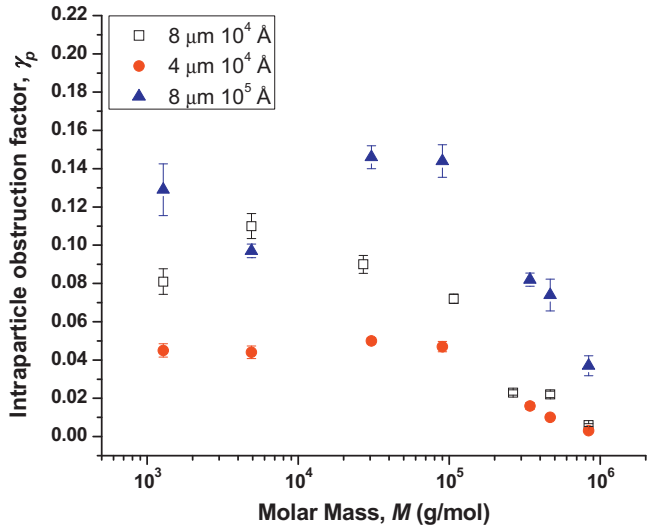

Fig. 2. Effect of molar mass, particle size, and pore size on the intraparticle obstruction factor γ_p of PMMA in THF at 30 °C.

generally exhibiting a maximum at $M \approx 30{,}000$ g/mol. A maximum is expected, due to the counterbalancing effects of K_{SEC} and D_m on γ_p. As M increases (i.e., as the polymer increases in size), D_m decreases. The mutual scaling of diffusion coefficient and molar mass, for both PS in THF and $CHCl_3$ and for PMMA in THF, is given by the approximate relation $D_m \propto (1/\sqrt{M})$ (see Eqs. (8)–(10)). Therefore, we can express the scaling relationship between γ_p, K_{SEC}, and M as $\gamma_p \propto K_{SEC}\sqrt{M}$. Starting at the highest molar mass examined, we observe the following behavior as a function of decreasing M: when the molar mass is large (relative to the exclusion limit of the column), K_{SEC} is consequently small (close to zero) and dominates the change in the value of γ_p (also close to zero). As molar mass decreases, K_{SEC} increases (begins to approach 1), causing γ_p to increase, and the term that eventually dominates the relation is $\sqrt{M}$. As M continues to decrease, the decrease in the $\sqrt{M}$ term for analytes with K_{SEC} close to unity results in an accompanying decrease in γ_p. The competing effects of K_{SEC} and M thus result in a maximum in the relationship between γ_p and M.

Similar behavior to that described above has been observed previously for low molar mass analytes [14,30]. Recently, Gritti and Guiochon noted that a maximum in the resistance to mass transfer through porous particles can be ascribed to the balance that exists between the influence of increasing accessible pore volume and the influence of increasing D_m with decreasing M [16].

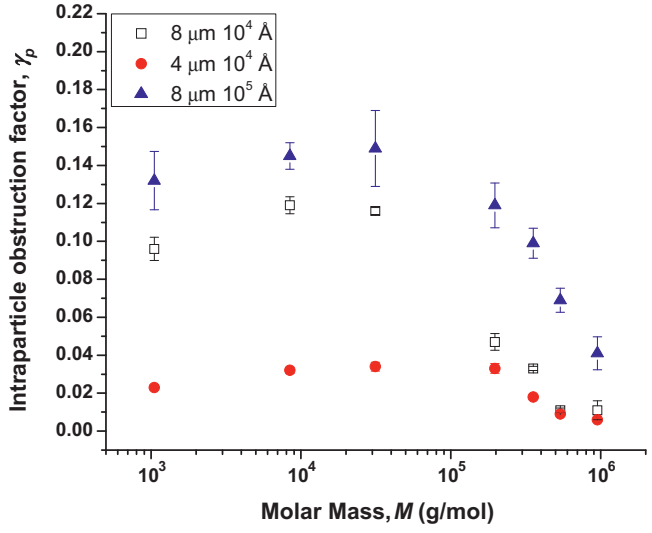

Fig. 3. Effect of molar mass, particle size, and pore size on the intraparticle obstruction factor γ_p of PS in $CHCl_3$ at 30 °C.

It should be noted that the maximum in the γ_p versus M plots occurs at lower M than predicted by the simple relation $\gamma_p \propto K_{SEC}\sqrt{M}$. The reason is that this relation ignores the effect of the $\partial\sigma^2_{perm}/\partial u$ term, the change in peak variance as a function of flow rate, in Eq. (7) on γ_p. Changes in peak variance depend on the size of the molecules in solution. All other things being equal, as an analyte becomes larger its diffusion coefficient becomes smaller, and a smaller diffusion coefficient results in slower partitioning of the analyte into and out of the pores of the packing material. This slow diffusion affects intraparticle mass transfer (C_{SM}-term broadening) and, because mass transfer is directly proportional to flow rate, as flow rate increases larger polymers exibit more band broadening than do smaller ones. This causes σ^2_{perm} to increase as a function of polymer size and $\partial\sigma^2_{perm}/\partial u$ to increase with increasing M. The intraparticle obstruction factor thus decreases with increasing M (beyond a given value of M, in our case ~30,000 g/mol) for two reasons, because of the decrease in K_{SEC} and because of the increase in $\partial\sigma^2_{perm}/\partial u$, both with increasing M.

4.3. Effect of analyte chemistry on γ_p

To examine the influence of repeat unit chemistry on γ_p, we compared our results for PS to those for a series of PMMAs. We chose PMMA due to the commercial availability of well-characterized narrow dispersity PMMA standards that cover the same broad M range examined for PS (roughly 1×10^3 to 1×10^6 g/mol). Additionally, PMMA can be analyzed at the same solvent and temperature conditions as PS.

The data in Tables 1–3 and Figs. 1–3 show the difference between the intraparticle obstruction factors of PS and those of PMMA under identical experimental conditions. For PS and PMMA of similar M, minor differences in γ_p are observed, with the obstruction factor of PMMA usually being slightly smaller than that of a similar-M PS. Because, at the experimental conditions employed, both the D_m and K_{SEC} of PMMA and PS are almost identical to each other, the observed differences in γ_p are seen to be due to the measured larger (by ~10–20%) change in peak variance with a change in flow rate (larger $\partial\sigma^2_{perm}/\partial u$ term in Eq. (7)) for PMMA as compared to PS. We are, at present, unable to explain the molecular-level basis of this difference.

As our results for γ_p rely on previously-reported D_m versus M relations, it seems appropriate to comment on the latter. For PS in THF, we chose to use the data set by Wernert et al. [27], as it appears to be the most recent and complete set, appearing in the literature earlier this year and covering the entire M range of our study (we had less choice when trying to find D_m versus M relations for PMMA in THF or PS in $CHCl_3$). We note, however, that we also calculated γ_p using three other sets of literature data [28,32,33]. In all cases, we found statistically significant differences between the γ_p values of PS and those of PMMA in THF at 30 °C. While all three sets produced similar results, the data set by Wernert et al. actually gave γ_p values for PS that were closest to those for PMMA, i.e., even larger differences between the intraparticle obstruction factors of PS and PMMA in THF at 30 °C are obtained using the data sets in Refs. [28,32,33].

4.4. Effect of solvent on γ_p

To investigate the effect of solvent on γ_p, we compared results obtained for PS in THF at both 30 and 50 °C to results obtained in $CHCl_3$ at the same temperatures and under otherwise identi-

cal conditions (i.e., same concentration and injection volume, same colums, etc.). We chose $CHCl_3$ for comparison because, as is the case for THF, $CHCl_3$ is a thermodynamically good solvent for PS and one in which the relationship beween M and D_m for PS can be derived from literature data (see Eqs. (10) and (11)).

As seen in Figs. 1 and 3 and Tables 1–3, the γ_p versus M relationship follows a similar trend in $CHCl_3$ as it does in THF. For the same M, however, the values of γ_p are generally lower in $CHCl_3$ than they are in THF. This is a direct result of the relation between D_m and M for PS in both solvents, given in Eqs. (8) and (10), respectively: The diffusion coefficient of a PS of a given M is lower in $CHCl_3$ at a given temperature than it is in THF at the same temperature. This lower D_m results in slower partitioning of the analyte into and out of the pores of the column packing when operating in $CHCl_3$, i.e., it corresponds to higher resistance to mass transfer (larger C_{SM} term in Eq. (1)) in $CHCl_3$ than in THF. The increase in band broadening that accompanies increased resistance to mass transfer (to which the difference between the viscosities of THF and $CHCl_3$ at a given temperature contributes), coupled with the increase in resistance to mass transfer that accompanies an increase in flow rate, causes peak variance to increase with increasing flow rate, more so in $CHCl_3$ than in THF (i.e., the $\partial\sigma^2_{\text{perm}}/\partial u$ term in Eq. (7) is larger in $CHCl_3$ than in THF). This, in turn, results in a higher γ_p for PS in THF than in $CHCl_3$.

It should be noted that the differences observed for γ_p in $CHCl_3$ versus THF are not due to preferential swelling of the column packing material in one solvent versus the other. We were able to rule out this possibility by noting that the ratio of system backpressures when operating in $CHCl_3$ and in THF at 30 °C was the same as the ratio of the 30 °C viscosities of these solvents. This was true at all five flow rates examined.

Not examined here were the effects, if any, on γ_p resultant from using solvents with different solvating power or, more accurately, of employing very thermodynamically different solvent/temperature conditions.

4.5. Effect of temperature on γ_p

The relationship between the intraparticle obstruction factor and temperature was examined by conducting experiments with PS in both THF and $CHCl_3$ at two different temperatures, 30 °C and 50 °C, the latter being the upper temperature limit of the instrumentation in our laboratory. When comparing the data obtained at these two temperatures, the values of γ_p for each molar mass at each temperature were generally within experimental error of each other (see Table 1). As such, it would appear that relatively modest (∼20 °C) changes in temperature cause no significant change in the values of the intraparticle obstruction factor. Because temperature affects both solvent viscosity and polymer size in solution, it would appear worthwhile to investigate the effect of temperature further using instrumentation with a higher upper temperature limit than the equipment presently available to us.

4.6. Effect of particle size on γ_p

To determine what effect, if any, column packing particle size has on γ_p we compared, under otherwise identical conditions, two columns of equal pore size (i.e., which separate over the same molar mass range for linear PS, or over the same size range in general) but which differed in particle size by a factor of two. The pore size of both columns was 10^4 Å, the "nominal" particle sizes 5 and 10 μm. As mentioned in Section 3.2, the actual particle sizes of these columns are 4 and 8 μm, respectively.

The smaller plate height afforded by smaller particles corresponds to less band broadening in the column packed with 4 μm particles as compared to the column packed with 8 μm particles. It also corresponds to a slower change in peak variance with changing flow rate (smaller $\partial\sigma^2_{\text{perm}}/\partial u$) for the column packed with smaller particles. This alone would tend to make γ_p larger for a given analyte in a column packed with smaller particles. However, as seen in Figs. 1–3 and when comparing to each other the data in Tables 1 and 2, we actually observe the opposite of this for PS and PMMA in THF and for PS in $CHCl_3$: in all circumstances, the experimentally-determined intraparticle obstruction factor is larger in the column packed with larger particles. To explain this result, we hypothesize as follows.

First, it should be noted that the retention volumes and distribution coefficients of the analytes are essentially the same in both columns. This indicates that both column have virtually identical pore volumes, as the interstitial volume of a column filled with identically well-packed spherical particles of homogeneous size is constant [3,34], regardless of the size of the particles. Also, the porosities of both columns are nearly identical (∼0.3% difference).

It has been known for several decades that, for linear random coils, the dependence of the distribution coefficient on the ratio of molecular size to pore size does not quantitatively agree with theoretical predictions that assume the shape of the pores to be either slab-shaped, cylindrical, or spherical (this matter is reviewed in more detail in Section 2.5.3 of Ref. [2]). Results from mercury porosimetry experiments on porous glass SEC packings suggest the presence of "ink bottle" structures in the packings [2,35,36]. If this is so, then the actual pore size of the packing material is underestimated, either by mercury intrusion or by the inverse SEC methods commonly used to determine the pore size distribution of polymeric (*e.g.*, styrene/divinylbenzene) packings [2]. The pore size reported by the manufacturers is based on the lowest molar mass PS standard that is totally excluded from the pores. This, however, only means that the PS standard is slightly larger than the narrow entrance of ink bottle pores, not necessarily larger than the internal cavity. If the larger-diameter (8 μm) packing particles in our study have larger "ink bottle" pores, of equal entrance size, to those in the smaller-diamater (4 μm) packing material, polymers will have the same access to the pores but, once inside the pores, there will be less obstruction to diffusion (larger γ_p) in the 8 μm as compared to the 4 μm particles. Pore volume and porosity should remain virtually identical, however, with retention volumes and distribution coefficients remaining constant regardless of particle size. The postulated hypothesis based on an ink bottle pore structure reconciles our results for particle size, pore size, retention volume, distribution coefficient, pore volume, porosity, and intraparticle obstructivity with the hysteresis loops previously observed in the mercury porosimetry experiments of Yau and Malone.

4.7. Effect of pore size on γ_p

To determine the effect of pore size on γ_p we compared, under otherwise identical conditions, two columns of the same particle size but which differed from each other with respect to pore size. Both columns were packed with 8 μm particles (nominal particle size, 10 μm). One column had a pore size of 10^4 Å and the other a pore size of 10^5 Å (as noted in the previous section, it is quite possible these pore size values represent the sizes of the entrances of pores with an ink bottle structure).

As seen in Figs. 1–3 and Tables 1 and 3, the analytes experience less intraparticle obstruction (larger γ_p) in the column packed with larger pore size particles. There are two reasons for this. First, for a column packed with large pore size particles, there is a greater difference between the volume occupied by the polymer in solution and the pore volume than there is for a column packed with particles with smaller pores. Qualitatively, the larger intraparticle (i.e., pore) volume available to the analyte means that the larger pores resemble the open tube scenario more so than do the smaller pores.

Quantitatively, this corresponds to a larger K_{SEC} for the analyte in the column packed with large pore size particles, as compared to the K_{SEC} in the small pore size column. Second, larger pores diminish the resistance to stagnant mobile phase mass transfer of the analyte, resulting in decreased band broadening and in a slower change in peak variance with changing flow rate (smaller $\partial\sigma^2_{\text{perm}}/\partial u$). As given by Eq. (7), both the larger K_{SEC} and the smaller $\partial\sigma^2_{\text{perm}}/\partial u$ contribute to the larger value of γ_p for the larger pore size column. Gritti and Guiochon have reported on the increase in intraparticle obstruction of reversed-phase columns with increasing stationary phase density [37]. As more stationary phase was present within silica particles, the volume of liquid available within the particles decreased. As pore volume lowered, intraparticle obstruction increased (i.e., γ_p decreased).

5. Conclusions

Presented here are results of experiments quantitating the individual influence of various analyte and column properties and user-defined parameters on the intraparticle obstruction factor γ_p. Due to the non-interacting nature of the column packing material used in size-exclusion chromatography, SEC proved to be a convenient technique through which to isolate the effects of the various parameters and properties studied on γ_p.

Far from being a constant, our experiments show that intraparticle obstructivity depends on a number of factors. The intraparticle obstruction factor was seen to be both molar mass and analyte dependent, with γ_p exhibiting a maximum with M that depends, qualitatively, on the balance between K_{SEC} and D_m.

We also investigated the effect of both solvent and temperature on γ_p. Smaller γ_p were observed in chloroform, where PS has a lower diffusion coefficient, than in THF at the same temperature. However, over the temperature range accessible to our equipment, we were not able to measure a statistically significant change in γ_p with temperature. Because temperature can affect both solvent viscosity and polymer size in solution, we encourage continued investigation into the effects of this parameter on γ_p.

Analyte repeat unit chemistry and molar mass are properties of the analyte, while solvent and temperature are parameters that are under the control of the user. We also examined the influence of column properties on γ_p. To this effect, we observed more intraparticle obstruction in columns packed with smaller particles and less intraparticle obstruction in columns packed with larger pore size packings, all other factors being equal. Our results, seemingly counterintuitive in the case of particle size, agree with a previously postulated ink bottle structure of pores in the column packing material.

While obtained via SEC, the results presented should be applicable to other forms of chromatography as well and should provide for a deeper understanding of the processes responsible for band broadening in column chromatography. Apposite to SEC, our results should aid in reducing the error associated with the various molar mass averages and distribution of polymers, as a result of the application of peak-position calibration curves to band broadened chromatographic peaks. The results and conclusions should also find value with those working in fields where an understanding of flow through porous media is important. Examples of the latter are the oil industry, where it is important to understand the diffusion of large molar mass crude oil products through porous rock formations [38], or the biochemical field, where an interest exists in understanding how large molar mass proteins diffuse through living cells [39].

Current experiments in our laboratory are focusing on determining the interparticle obstruction factor γ_e and the relationship between γ_e, γ_p, and the total obstruction factor γ_t. We expect to report on these soon.

Acknowledgements

The authors would like to thank Agilent/Polymer Laboratories for a donation of two PLgel SEC columns for this research. We would also like to thank Professor John G. Dorsey (Department of Chemistry & Biochemistry, Florida State University) for helpful advice and discussions.

References

[1] J.J. van Deemter, F.J. Zuiderweg, A. Klinkenberg, Chem. Eng. Sci. 5 (1956) 271.
[2] A.M. Striegel, W.W. Yau, J.J. Kirkland, D.D. Bly, Modern Size-Exclusion Liquid Chromatography, 2nd ed., Wiley, New York, 2009.
[3] J.C. Giddings, Dynamics of Chromatography. Principles and Theory, Marcel Dekker, New York, 1965.
[4] A.M. Striegel, J. Chromatogr. A 932 (2001) 21.
[5] A.M. Striegel, J. Am. Chem. Soc. 125 (2003) 4146 (See Erratum in J. Am. Chem. Soc. 126 (2004) 4740).
[6] M.A. Boone, H. Nymeyer, A.M. Striegel, Carbohydr. Res. 343 (2008) 132.
[7] A.M. Striegel, Anal. Chem. 77 (2005) 104A.
[8] A.M. Striegel (Ed.), Multiple Detection in Size-Exclusion Chromatorgraphy, American Chemical Society, Washington, DC, 2005.
[9] A.M. Striegel, Anal. Bioanal. Chem. 390 (2008) 303.
[10] L.R. Snyder, J.J. Kirkland, J.W. Dolan, Introduction to Modern Liquid Chromatography, 3rd ed., Wiley, New York, 2010.
[11] H. Pasch, B. Trathnigg, HPLC of Polymers, Springer, Berlin, 1999.
[12] J.C. Giddings, K.L. Mallik, Anal. Chem. 38 (1966) 997.
[13] J.C. Giddings, J. Bowman, M. Lyle, M.N. Myers, Macromolecules 10 (1976) 443.
[14] J. Klein, M. Grüneberg, Macromolecules 14 (1981) 1411.
[15] M. Potschka, J. Chromatogr. 648 (1993) 41.
[16] F. Gritti, G. Guiochon, Anal. Chem. 79 (2007) 3188.
[17] A.M. Striegel, J. Chromatogr. A 1033 (2004) 241.
[18] A.E. Scheidegger, The Physics of Flow Through Porous Media, University of Toronto Press, Toronto, 1960.
[19] A.G. Hunt, Percolation Theory for Flow in Porous Media, Springer, Berlin, 2005.
[20] J.J. Kirkland, W.W. Yau, H.J. Stoklosa, C.H. Dilks Jr., J. Chromatogr. Sci. 15 (1977) 303.
[21] W.W. Yau, Anal. Chem. 49 (1977) 395.
[22] J.P. Foley, J.G. Dorsey, Anal. Chem. 55 (1983) 730.
[23] K. Matyjasezewski, T.P. Davis, Handbook of Radical Polymerization, Wiley, New York, 2002.
[24] L. Pasti, F. Dondi, M. van Hulst, P.J. Schoenmakers, M. Martin, A. Felinger, Chromatographia Suppl. 57 (2003) S-171.
[25] M.A. Boone, A.M. Striegel, Macromolecules 39 (2006) 4128.
[26] T.D. Buley, A.M. Striegel, Carbohydr. Polym. 79 (2010) 241.
[27] V. Wernert, R. Bouchet, R. Denoyel, Anal. Chem. 82 (2010) 2668.
[28] M.E. Schimpf, J.C. Giddings, J. Polym. Sci. B: Polym. Phys. 27 (1989) 1317.
[29] K. Dehara, T. Yoshizaki, H. Yamakawa, Macromolecules 26 (1993) 5137.
[30] C.K. Colton, C.N. Satterfield, C.-J. Lai, AIChE J. 21 (1975) 289.
[31] A. Berthod, F. Chartier, J.-L. Rocca, J. Chromatogr. 469 (1989) 53.
[32] E.P.C. Mes, W.Th. Kok, H. Poppe, R. Tijssen, J. Polym. Sci. B: Polym. Phys. 37 (1999) 593.
[33] W. Mendema, H. Zeldenrust, Polymer 18 (1977) 835.
[34] D.J. Cumberland, R.J. Crawford, The Packing of Particles, Elsevier, Amsterdam, 1987.
[35] W.W. Yau, C.P. Malone, Polym. Prepr. 12 (1977) 797.
[36] J.W. McBain, J. Am. Chem. Soc. 57 (1935) 699.
[37] F. Gritti, G. Guiochon, Chem. Eng. Sci. 61 (2006) 7636.
[38] M.A. Mohammed, J. Appl. Polym. Sci. 110 (2008) 1382.
[39] J.A. Dix, A.S. Verkman, Ann. Rev. Biophys. 37 (2008) 247.